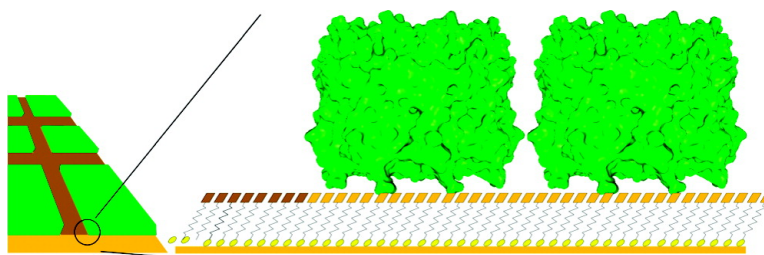


## Directed Formation of Micro- and Nanoscale Patterns of Functional Light-Harvesting LH2 Complexes

Nicholas P. Reynolds, Stefan Janusz, Maryana Escalante-Marun, John Timney, Robert E. Ducker, John D. Olsen, Cees Otto, Vinod Subramaniam, Graham J. Leggett, and C. Neil Hunter

*J. Am. Chem. Soc.*, **2007**, 129 (47), 14625-14631 • DOI: 10.1021/ja073658m

Downloaded from <http://pubs.acs.org> on February 9, 2009



### More About This Article

Additional resources and features associated with this article are available within the HTML version:

- Supporting Information
- Links to the 4 articles that cite this article, as of the time of this article download
- Access to high resolution figures
- Links to articles and content related to this article
- Copyright permission to reproduce figures and/or text from this article

[View the Full Text HTML](#)

## Directed Formation of Micro- and Nanoscale Patterns of Functional Light-Harvesting LH2 Complexes

Nicholas P. Reynolds,<sup>†</sup> Stefan Janusz,<sup>†</sup> Maryana Escalante-Marun,<sup>‡</sup> John Timney,<sup>§</sup>  
Robert E. Ducker,<sup>†</sup> John D. Olsen,<sup>§</sup> Cees Otto,<sup>‡</sup> Vinod Subramaniam,<sup>‡</sup>  
Graham J. Leggett,<sup>\*,†</sup> and C. Neil Hunter<sup>§</sup>

Contribution from the Department of Chemistry, University of Sheffield, Sheffield S3 7HF, U.K.,  
Department of Molecular Biology and Biotechnology, University of Sheffield, Sheffield S10 2TN,  
U.K., and Department of Science and Technology, MESA+ Institute for Nanotechnology, 7500  
AE Enschede, The Netherlands

Received May 22, 2007; E-mail: graham.leggett@shef.ac.uk

**Abstract:** The precision placement of the desired protein components on a suitable substrate is an essential prelude to any hybrid “biochip” device, but a second and equally important condition must also be met: the retention of full biological activity. Here we demonstrate the selective binding of an optically active membrane protein, the light-harvesting LH2 complex from *Rhodobacter sphaeroides*, to patterned self-assembled monolayers at the micron scale and the fabrication of nanometer-scale patterns of these molecules using near-field photolithographic methods. In contrast to plasma proteins, which are reversibly adsorbed on many surfaces, the LH2 complex is readily patterned simply by spatial control of surface polarity. Near-field photolithography has yielded rows of light-harvesting complexes only 98 nm wide. Retention of the native optical properties of patterned LH2 molecules was demonstrated using in situ fluorescence emission spectroscopy.

### Introduction

Membrane proteins such as energy- and electron-transfer complexes, shuttles, and pumps possess many desirable traits for the emerging field of bionanotechnology since they have evolved the capacity to absorb, transmit, and interconvert various forms of free energy, for example, electromagnetic radiation, redox potentials, proton and ion gradients. Examples of biological processes that harness these properties include photosynthesis and signal transduction at nerve synapses. Photosynthetic membrane proteins are particularly interesting since they operate on timescales ranging from femtoseconds to milliseconds, and with extraordinarily high efficiencies.

The use of proteins for bionanotechnology and bioelectronics has been reviewed,<sup>1</sup> and there are many reports of attaching functional photosynthetic complexes to various types of electrodes.<sup>2–4</sup> Patterning of proteins on the microscale has been demonstrated by a variety of means, for example, using microcontact printing,<sup>5–8</sup> but despite much effort, nanometer-scale patterning of proteins of any type remains challenging,

and there are few published reports of sub-100 nm protein patterns. The most successful approaches to date have been based upon dip pen nanolithography<sup>9–12</sup> and conductive atomic force microscopy (AFM) lithography.<sup>13</sup> Recently, photolithographic patterning<sup>14–17</sup> of self-assembled monolayers (SAMs) has been successfully used to direct the immobilization of plasma proteins with a precision of ca. 50 nm.<sup>18</sup> Given the importance of membrane proteins as a class of biomolecule, and the explosion of interest in bionanotechnology, the development of reliable methods for the fabrication of membrane protein structures approaching molecular dimensions is an important goal.

At a fundamental level, while much is known about the adsorption of plasma proteins to solid surfaces, a great deal less

<sup>†</sup> Department of Chemistry, University of Sheffield.

<sup>§</sup> Department of Molecular Biology and Biotechnology, University of Sheffield.

<sup>‡</sup> MESA+ Institute for Nanotechnology.

- (1) Davis, J. J.; D. A. M.; Wrathmell, C. L.; Axford, D. N.; Zhao, J.; Wang, N. *J. Mater. Chem.* **2005**, *15*, 2160.
- (2) Ogawa, M.; Kanda, R.; Dewa, T.; Iida, K.; Nango, M. *Chem. Lett.* **2002**, *31*, 466.
- (3) Trammella, S. A.; L. W.; Zulloa, J. M.; Shashidharb, R.; Lebedev, N. *Biosens. Bioelectron.* **2004**, *19*, 1649.
- (4) Lebedev, N.; Trammell, S. A.; Spano, A.; Lukashov, E.; Griva, I.; Schnur, J. *J. Am. Chem. Soc.* **2006**, *128*, 12044.

- (5) Tan, J. L.; Tien, J.; Chen, C. S. *Langmuir* **2002**, *18*, 519.
- (6) Lopez, G. P.; Biebuyck, H. A.; Haerter, R.; Kumar, A.; Whitesides, G. M. *J. Am. Chem. Soc.* **1993**, *115*, 10774.
- (7) Ye Fang, A. G. F.; Lahiri, J. *J. Am. Chem. Soc.* **2002**, *124*, 2394.
- (8) Lopez, G. P.; Albers, M. W.; Schreiber, S. L.; Carroll, R.; Peralta, E.; Whitesides, G. M. *J. Am. Chem. Soc.* **2003**, *115*, 5877.
- (9) Lee, K.-B.; Park, S.-J.; Mirkin, C. A.; Smith, J. C.; Mirsich, M. *Science* **2002**, *295*, 1702.
- (10) Lee, K.-B.; Lim, J.-H.; Mirkin, C. A. *J. Am. Chem. Soc.* **2003**, *125*, 5588.
- (11) Hyun, J.; Ahn, S. J.; Lee, W. K.; Chilkoti, A.; Zauscher, S. *Nano Lett.* **2002**, *2*, 1203.
- (12) Nam, J.-W.; Han, S. W.; Lee, K.-B.; Liu, X.; Ratner, M. A.; Mirkin, C. A. *Angew. Chem., Int. Ed.* **2004**, *43*, 1246.
- (13) Gu, J.; Yam, C. M.; Li, S.; Cai, C. *J. Am. Chem. Soc.* **2004**, *126*, 8098.
- (14) Sun, S.; Chong, K. S. L.; Leggett, G. J. *J. Am. Chem. Soc.* **2002**, *124*, 2414.
- (15) Sun, S.; Leggett, G. J. *Nano Lett.* **2004**, *4*, 1381.
- (16) Sun, S.; Montague, M.; Critchley, K.; Chen, M.-S.; Dressick, W. J.; Evans, S. D.; Leggett, G. J. *Nano Lett.* **2006**, *6*, 29.
- (17) Leggett, G. J. *Chem. Soc. Rev.* **2006**, *35*, 1150.
- (18) Montague, M.; Ducker, R. E.; Chong, K. S. L.; Manning, R. J.; Rutten, F. J. M.; Davies, M. C.; Leggett, G. J. *Langmuir* **2007**, *23*, 7328.

is known about the adsorption of membrane proteins. For example, oligo(ethylene glycol) terminated monolayers have been widely used to resist the adsorption of plasma proteins,<sup>19–23</sup> and the mechanism of protein resistance has been the subject of vigorous debate. However, there have been few systematic studies of membrane protein adsorption.

The combination of patterning and demonstration of biological activity for membrane proteins is thus elusive. In this work, we examine the suitability of a particular photosynthetic light-harvesting complex, termed LH2, for controlled deposition onto a self-assembled monolayer (SAM). LH2 is a cylindrical membrane protein complex with an external diameter of  $\sim 7$  nm and height of  $\sim 7$  nm, which contains two circular rings of 9 and 18 bacteriochlorophyll molecules.<sup>24,25</sup> The LH2 complex of the photosynthetic bacterium *Rhodobacter sphaeroides* is used here due to the ease of production of highly purified protein, its excellent physical stability, its well-documented spectral properties, and its amenability to genetic and biochemical manipulation.<sup>26,27</sup> The objective is to exert spatial control over the positioning of LH2 complexes so that they cluster to form micro- and nanoscale patterns while retaining their biological function, as determined by optical spectroscopy. Biological aims of such work include examining energy migration in artificially constructed, extended arrays of LH complexes. In the native membrane bilayer, these arrays comprise several thousand interconnected bacteriochlorophyll molecules that form a single energy transfer domain.<sup>28</sup> Such work requires control and consistency of orientation of LH complexes on supports which tether the complexes, as well as the ability to impose defined sizes and shapes to the energy transfer domains. Finally, it is essential that the patterned LH complexes retain their functionality on the solid support, something that is readily verified in the case of LH complexes by in situ measurement of their fluorescence emission properties. This paper demonstrates the patterning of LH2 and retention of its native optical properties.

Figure 1 shows, schematically, the method that we have explored. A monolayer of protein-resistant adsorbates (for example, a perfluorinated thiol) is formed on gold and selectively exposed to UV illumination, leading to photochemical conversion of the alkylthiolate adsorbate complexes to weakly bound alkylsulfonates. Exposure to light through a mask yields micrometer-scale patterns, while exposure to the evanescent field associated with a scanning near-field optical microscope probe may be used to form nanostructures. The sample is then immersed in a solution of a carboxylic acid terminated thiol to which the protein is covalently immobilized by activating the acid groups to render them reactive toward lysine residues on

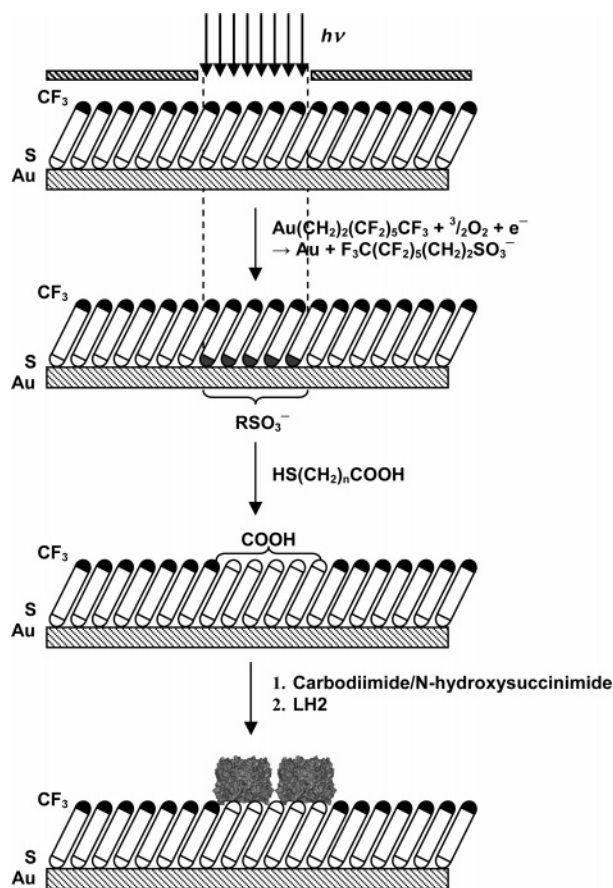


**Figure 1.** Schematic diagram showing the photopatterning of protein-resistant self-assembled monolayers, and the subsequent activation of carboxylic acid groups and immobilization of LH2.

the cytoplasmic face of the light-harvesting complex. Self-assembled monolayers (SAMs) were surveyed for their suitability to resist the adsorption of LH2, and covalent attachment of the protein to activated monolayers confirmed using surface plasmon resonance. Nanoscale structures were formed using scanning near-field photolithography (SNP).<sup>14–17</sup> The in situ fluorescence properties of LH2 were measured, and the observation of qualitatively identical spectra for solution-phase and patterned proteins demonstrates retention of its native function.

## Experimental Section

**Purification of WT-LH2.** The LH2 complex was purified from wild-type *Rba. sphaeroides* 2.4.1., which was photosynthetically grown under low light ( $5 \text{ W m}^{-2}$ ) illumination. The purification of the LH2 complex from this strain was carried out as follows. Cells were disrupted using a French press at a pressure of 18 000 psi. Unbroken cells and cell debris were removed by centrifugation (100 000g for 30 min). The supernatant containing the intracytoplasmic membrane (ICM) fraction was pelleted by centrifugation at 200 000g for 2 h and then resuspended in working buffer, 20 mM Tris at pH 8. Membranes were solubilized with 4% *N,N*-dimethyldodecylamine-*N*-oxide (LDAO) for 45 min. Insoluble material was removed by centrifugation at 200 000g for 1 h. The solubilized LH2 was then applied to a DEAE (Sigma) ion exchange column and eluted using a 0–250 mM NaCl gradient, in working buffer plus 0.1% LDAO. The LH2 was then applied to a Resource Q column (GE Healthcare) with a 0–500 mM NaCl gradient, in working buffer plus 0.1% LDAO. The LH2 complex eluting at  $\sim 300$  mM NaCl was collected, concentrated, and applied to a Superdex 200 gel filtration column (GE Healthcare). Eluted fractions having an A850/A280 absorbance ratio greater than 3.4 were pooled and concentrated. LH2

- (19) Prime, K. L.; Whitesides, G. M. *Science* **1991**, *252*, 1164.  
 (20) Dicke, C.; Haehner, G. *J. Am. Chem. Soc.* **2001**, *124*, 12619.  
 (21) Mrksich, M.; Sigal, G. B.; Whitesides, G. M. *Langmuir* **1995**, *11*, 4383.  
 (22) Harder, P.; Grunze, M.; Dahint, R.; Whitesides, G. M.; Laibinis, P. E. *J. Phys. Chem. B* **1998**, *102*, 426.  
 (23) Ostuni, E.; Chapman, R. G.; Holmlin, E. R.; Takayama, S.; Whitesides, G. M. *Langmuir* **2001**, *17*, 5605.  
 (24) McDermott, G. P.; Prince, S. M.; Freer, A. A.; Hawthornthwaite-Lawless, A. M.; Papiz, M. Z.; Cogdell, R. J.; Isaacs, N. W. *Nature* **1995**, *374*, 517.  
 (25) Koepke, J.; Xu, H.; Muenke, C.; Schulten, K.; Michel, H. *Structure* **1996**, *4*, 581.  
 (26) Walz, T.; Jamieson, S. J.; Bowers, C. M.; Bullough, P. A.; Hunter, C. N. *J. Mol. Biol.* **1998**, *282*, 833.  
 (27) Fowler, G. J. S.; Visschers, R. W.; Grief, G. G.; van Grondelle, R.; Hunter, C. N. *Nature* **1992**, *355*, 848.  
 (28) Vos, M. H.; van Dorssen, R. J.; Amez, J.; van Grondelle, R.; Hunter, C. N. *Biochim. Biophys. Acta* **1988**, *933*, 132.

sample homogeneity was established by SDS–PAGE and electrospray mass spectroscopy.

**Preparation of Monolayers.** Self-assembled monolayers were formed following well-established procedures,<sup>29,30</sup> by the immersion of gold-coated substrates in 1 mM solutions of the appropriate thiol (Sigma Chemical Company, Poole, UK) in ethanol for 18 h. (1-Mercaptoundec-11-yl)tri(ethylene glycol) ( $C_{11}(\text{OEG})_3$ ) was synthesized according to a method previously published by Pale-Grosdemange et al.<sup>31</sup> All glassware was cleaned using Piranha solution (70:30). Substrates were prepared by the evaporation of gold (20 nm) onto chromium-primed (2 nm) glass cover slips (Chance Proper no. 2 thickness, size 22 mm × 64 mm). Atomic force microscopy measurements were made using a Digital Instruments Nanoscope III Multimode AFM (Veeco, Cambridge, UK).

**Lithography.** Photopatterning was conducted using light from a frequency-doubled argon ion laser (Coherent FreD 300C, Coherent UK, Ely) which emits at 244 nm. For micron-scale patterning, 2000 and 1500 mesh electron microscope grids (consisting of  $12.7 \times 12.7$  and  $16.9 \times 16.9 \mu\text{m}^2$  square openings, respectively) were used as masks, and the sample was irradiated at a laser power of 100 mW. The power incident on the surface was ca. 68% of the laser power, and the irradiation time was typically 12 min. The illuminated area was 0.2–0.4 cm<sup>2</sup>, meaning that the incident power was 170–340 mW cm<sup>-2</sup>, and the net exposure at the surface was in the range of 20–40 J cm<sup>-2</sup>, comfortably in excess of the exposure required to ensure complete photo-oxidation of the adsorbates.<sup>32</sup> The samples were then immersed in a solution of a second thiol to displace the oxidation products and adsorb at the surface, forming a molecular pattern. For scanning near-field photolithography, the laser was coupled to a ThermoMicroscopes Aurora III near-field scanning optical microscope fitted with a probe formed by etching a fused silica fiber probe in HF and depositing an Al coating onto the cone. An aperture was formed by gently colliding the probe with a surface. During near-field lithography, the probe velocity was  $0.1 \mu\text{m s}^{-1}$  during fabrication of lines. Spots were fabricated using a stationary probe with an exposure time of 4 s. Following exposure in the near field, samples were then immersed in a solution of a second thiol, which displaced the oxidation products, and then rinsed with ethanol and dried.

**Protein Immobilization.** Samples were exposed to solutions of LH2 ( $6.5 \mu\text{g mL}^{-1}$  in a buffer consisting of 10 mM Tris (pH 7.4) and 150 mM KCl) for 15 min. The sample was rinsed with buffer to remove any unbound LH2 and either characterized using surface plasmon resonance or imaged using AFM or optical microscopy. To achieve a covalent bond between the carboxylic acid terminated SAM and the LH2 complexes, the SAM was first activated to form surface-bound *N*-hydroxysuccinimidyl esters by exposure of the sample to an aqueous solution of *N*-hydroxysuccinimide (Sigma) (20 mM) and 1-ethyl-3,3-dimethyl carbodiimide (Sigma) (20 mM).<sup>18,33</sup>

**Optical Microscopy.** Patterned LH2 was imaged using an inverted confocal laser scanning microscope. The confocal microscope is a home-built device using a diode laser light source (Roithner Laser Technik, RLT80010MG,  $\lambda = 800$  nm) reflected via a dichroic beam splitter (Chroma, Q850LPXXR) to an oil immersion objective (Nikon, Plan Fluor 100×, NA 1.3) that focuses the light on the sample. The diode laser operates at an ideal wavelength to stimulate the B800 bacteriochlorophylls in the LH2. The same objective collects the fluorescence which passes through the dichroic beam splitter. A foldable mirror directs the fluorescence light to either single photon counting

avalanche photodiode (SPCM-AQR-14, Perkin-Elmer Optoelectronics) or a custom-designed prism-based spectrograph with single molecule sensitivity, equipped with a liquid nitrogen cooled CCD camera (Spec-10:100B, Princeton Instruments). Any remaining excitation light is removed from the detection path by a holographic notch filter (HNPF-800, Kaiser Optical Systems). The APD collects a high-resolution fluorescence image of the entire spectral range of the photodiode. Due to the much longer acquisition time of the CCD, the resolution was reduced when using this method to acquire spectra, but a complete emission spectrum was recorded for every pixel in the image.<sup>34</sup>

**Atomic Force Microscopy.** Tapping mode AFM images and friction force microscopy measurements were acquired on a Digital Instruments Nanoscope Multimode IIIa atomic force microscope (Digital Instruments, Cambridge, UK). In both cases, measurements were made in air. The probes used were silicon nitride nanoprobes (Digital Instruments, Cambridge, UK). The nominal force constants of these probes were 0.06 or 0.12 N m<sup>-1</sup> for the contact mode probes and 50 N m<sup>-1</sup> for the tapping mode probes.

## Results and Discussion

**Evaluation of Substrates for Binding the LH2 Light-Harvesting Complex.** The strategy explored in the present study was to pattern the chemical composition of the substrate, in order to control its adhesiveness toward LH2 in a localized fashion. While the adsorption of plasma proteins onto synthetic surfaces has been extensively studied, there are fewer reports of the adsorption of membrane proteins. Moreover, an additional difference in the present case is provided by the fact that the protein is stabilized by surfactants. It was necessary, therefore, to survey a range of synthetic surfaces for their adhesiveness toward proteins. Critically, it was important to identify a surface that resisted unwanted adsorption, given the large body of literature suggesting that in general protein adsorption onto most solid surfaces is rapid and irreversible. Self-assembled monolayers of mercaptoundecanoic acid ( $C_{10}\text{COOH}$ ), mercaptoundecanol ( $C_{11}\text{OH}$ ), and dodecanethiol ( $C_{11}\text{CH}_3$ ) were formed. These reflect a range of surface free energies and compositions and have been extensively studied. In addition, monolayers of the perfluorinated adsorbate,  $\text{HS}(\text{CH}_2)_2(\text{CF}_2)_5\text{CF}_3$  ( $\text{C}_2\text{F}_5\text{CF}_3$ ), were formed to provide a surface even more hydrophobic than  $C_{11}\text{CH}_3$ . Finally, monolayers of (1-mercaptoundec-11-yl)tri(ethylene glycol) ( $C_{11}(\text{OEG})_3$ ) were also used. Oligo(ethylene glycol) (OEG) terminated thiols, first pioneered by Whitesides and co-workers,<sup>6,21,23,31</sup> have been found to exhibit extreme resistance to the adsorption of plasma proteins and thus provide an important reference point for evaluating the behavior of membrane proteins.

Figure 2 shows surface plasmon resonance (SPR) data for the adsorption of LH2 onto these surfaces. Initially, the protein solution was injected and the signal monitored for 10 min. Buffer was then injected, and the signal was monitored for a further 3 min. Finally, a 0.5% solution of detergent, sodium dodecyl sulfate (SDS), was injected and the signal monitored for a further minute.

As expected,  $C_{11}(\text{OEG})_3$  (trace 6) proved strongly resistant to the adsorption of LH2. The initial increase in the SPR signal following introduction of the protein was close to the minimum detection limit, and the signal immediately returned to zero following introduction of buffer, indicating that the adsorbed material was only very weakly bound and readily displaced from

(29) Nuzzo, R. G.; Fusco, F. A.; Allara, D. L. *J. Am. Chem. Soc.* **1987**, *109*, 2358.

(30) Bain, C. D.; Troughton, E. B.; Tao, Y.-T.; Evall, J.; Whitesides, G. M.; Nuzzo, R. G. *J. Am. Chem. Soc.* **1989**, *111*, 321.

(31) Pale-Grosdemange, C.; Simon, E. S.; Prime, K. L.; Whitesides, G. M. *J. Am. Chem. Soc.* **1991**, *113*, 12.

(32) Brewer, N. J.; Janusz, S. J.; Critchley, K.; Evans, S. D.; Leggett, G. J. *J. Phys. Chem. B* **2005**, *109*, 11247.

(33) Patel, N.; Davies, M. C.; Hartshorne, M.; Heaton, R. J.; Roberts, C. J.; Tendler, S. J. B.; Williams, P. M. *Langmuir* **1997**, *13*, 6485.

(34) Kassies, R. V. D.; van der Werf, K. O.; Lenferink, A.; Hunter, C. N.; Olsen, J. D.; Subramaniam, V.; Otto, C. J. *Microscopy* **2005**, *217*, 109.

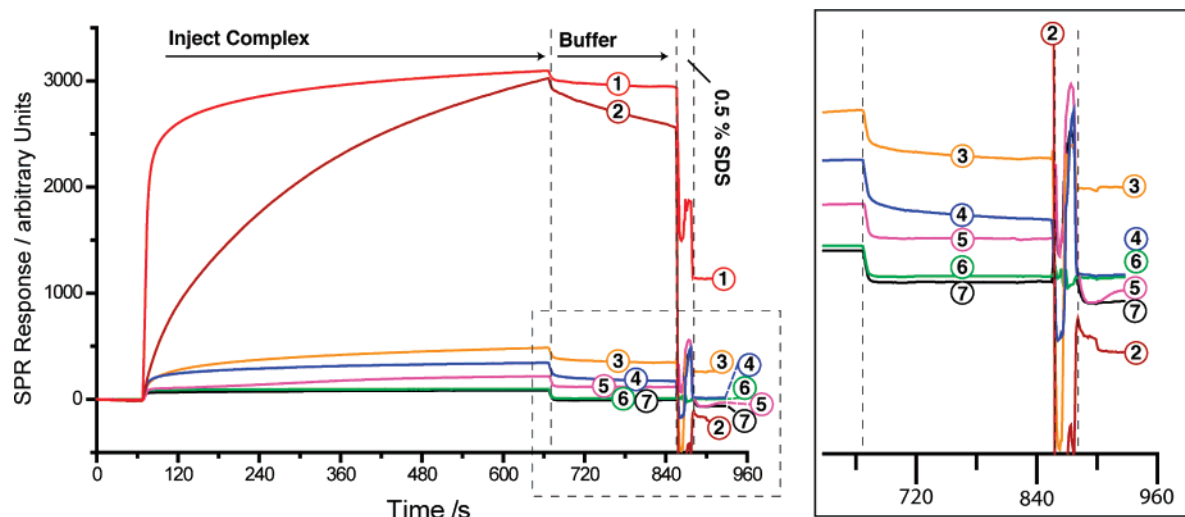


**Figure 2.** SPR sensorgrams of dynamic binding of the LH2 complex to a range of SAMs: (1)  $C_{10}COO$ -succinimide activated ester, (2)  $C_{10}COOH$ , (3) bare gold, (4)  $C_{11}OH$ , (5)  $C_{11}CH_3$ , (6)  $C_{11}(OCH_2)_3OH$ , (7)  $C_2F_5CF_3$ . The box on the right shows an expanded view of the region between 640 and 960 s.

the surface. Unexpectedly, an identical behavior was observed for LH2 on the  $C_2F_5CF_3$  surface (trace 7). While the low surface free energy of fluorinated surfaces is generally expected to render them comparatively resistant to adhesive interactions, substantial adsorption of plasma proteins, for example, is still observed. This is because the interaction of a protein with the surface leads gradually to the reorganization of its conformation to minimize the interfacial free energy.<sup>35</sup> This results in a substantial hydrophobic interaction that gradually renders the interaction irreversible. In the case of LH2, this plainly does not occur. We speculate that this may be due to the fact that the hydrophobic sides of LH2 are surrounded, in the present case, by detergent molecules, which, like the cytoplasmic and periplasmic regions of LH2, present a hydrophilic exterior to the solution phase and also provide stabilization to LH2. This belt of detergent molecules could reduce the propensity for conformational reorganization following adsorption of LH2 onto the hydrophobic surface. This in turn would reduce the chances of LH2 adsorbing onto the fluorinated surface.

Similar behavior was observed when  $C_{11}CH_3$  (trace 5) was used as the substrate for binding LH2. The SPR data suggested that some protein remained at the  $C_{11}CH_3$  surface (trace 5) following introduction of the buffer. However, this was a very small amount and was close to the limits of detection of SPR; moreover, on introduction of SDS, this protein was completely removed, indicating that the interaction with the surface is very weak indeed. Much the same was also true for the hydrophilic surface,  $C_{11}OH$  (trace 4): although a very small amount of protein remained after introduction of buffer, it was removed completely by SDS. Hence, even hydrophilic surfaces are not necessarily strongly binding toward LH2. However, a very different type of behavior was observed for  $C_{10}COOH$  (trace 2). For these surfaces, extensive adsorption occurred during the initial introduction of LH2, and little of this protein (less than 20%) was displaced from the surface following washing with buffer. These observations suggest that there is a very strong interaction between LH2 and carboxylate groups. Because there was little binding of LH2 to the other hydrophilic surface,  $C_{11}$ -

OH (trace 4), it is clearly not the surface free energy that is the driving force for this interaction. Given that the cytoplasmic face of LH2 is likely to be positively charged, the interaction between LH2 and  $C_{10}COOH$  (trace 2) is probably electrostatic in origin.

Introduction of SDS led to complete removal of LH2 from  $C_{10}COOH$  (trace 2). In order to ensure that a permanent interaction between the protein and the surface could be achieved for later patterning work,  $C_{10}COOH$  surfaces were activated using *N*-hydroxysuccinimide and 1-ethyl-3-(3-dimethyl carbodiimide), following well-established procedures,<sup>18,33</sup> in conjunction with photopatterning methods,<sup>18</sup> for the fabrication of nanostructured plasma proteins. The result of the activation process is the formation of active ester intermediates at the monolayer surface which react with free amine groups (from lysine residues on the protein) to form amide linkages. The high number of lysine residues, solely found on the cytoplasmic face of LH2, ensures adequate attachment and probably directs a consistent topology for bound complexes. Figure 2 provides clear evidence for the efficacy of this approach. After initial introduction of the protein, the SPR signal detected for the  $C_{10}COOH$  (trace 2) and the active ester (trace 1) surfaces was very similar. After introduction of buffer, there was a negligible reduction in the signal measured for the activated surface (trace 1). Following rinsing with SDS, the signal measured for the activated surface fell, but only to ca. 40% of the maximum value measured, indicating that a significant fraction of the adsorbed protein was, in fact, covalently attached. This contrasts strongly with the  $C_{10}COOH$  surface from which the LH2 was effectively removed.

**Directed Formation of Micron-Scale Patterns of LH2 Complexes on the Self-Assembled Monolayers.** Patterned SAMs were formed using photolithographic techniques. Micron-scale structures were formed by exposure of a  $C_2F_5CF_3$  monolayer to UV light through a mask. In exposed regions, the adsorbates were converted to sulfonate species which, unlike the thiols, are only weakly adsorbed to the gold surface.<sup>17</sup> The sample was then immersed in a solution of a contrasting adsorbate, in this case, a carboxylic acid terminated thiol, which displaced the oxidation products, adsorbing at the surface. The

(35) Brash, J. L., Horbett, T. A., Eds. *Proteins at Interfaces: Physicochemical and Biochemical Studies*; ACS Symposium Series 343; American Chemical Society: Washington, DC, 1987.

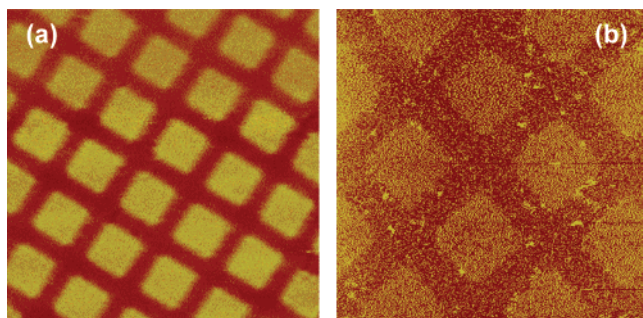


**Figure 3.** Images of a  $C_2F_5CF_3/C_{10}COOH$  pattern formed on a gold surface: (a) A  $100\ \mu\text{m} \times 100\ \mu\text{m}$  FFM image,  $z$ -range: 0–350 mV photodetector signal; (b)  $50\ \mu\text{m} \times 50\ \mu\text{m}$  tapping mode ( $z$ -scale range 0–15 nm) image of a similar pattern following conversion of the carboxylic acid groups to active esters and coupling of LH2.

result was a surface that consisted of square regions, which had been exposed to UV light through the mask, where the LH2-resistant  $C_2F_5CF_3$  adsorbate had been replaced by  $C_{10}COOH$ , while the original chemistry was retained in the regions masked during exposure. The sample was imaged using friction force microscopy (FFM) to examine the quality of the patterns. In FFM, lateral deflections of an atomic force microscope (AFM) cantilever are measured in contact mode.<sup>36</sup> These are strongly influenced by the strength of the frictional interaction between the tip and the surface.<sup>37–39</sup> The outer surface of a standard, commercially fabricated silicon nitride probe consists of polar silicon dioxide. A strong adhesive interaction and hence a large frictional force and bright contrast was thus observed as the tip slid across the polar regions. Figure 3a shows a representative image. The squares ( $C_{10}COOH$ ) exhibit bright contrast, whereas the fluorinated regions of the surface (bars) exhibit dark contrast because the tip adheres poorly to these regions.

The patterned surface was then activated by incubation with the carbodiimide/*N*-hydroxysuccinimide solution and, following activation (i.e., treatment identical to that used to generate trace 1 in Figure 2), it was transferred to a solution of LH2. The sample was removed after 20–30 min, rinsed with buffer, and examined using tapping mode AFM. Figure 3b shows a representative image of the sample topography. LH2 has attached extensively to the square regions, as expected, but very little protein has adsorbed to the  $C_2F_5CF_3$  regions (cf. trace 7 in Figure 2). The amount of nonspecific adsorption is not zero, but the extent is probably exaggerated in the image because of the broadening that occurs because of convolution of the profile of the AFM tip (which has a radius of curvature over twice the size of the protein) with the molecular structure. In Figure 2, protein adsorption on the  $C_2F_5CF_3$  SAM was not detected using SPR; hence, any nonspecifically adsorbed proteins in Figure 3b must be present at a surface concentration below the detection limit of SPR. The mean height of the square regions in the image in Figure 3b above the  $C_2F_5CF_3$  SAM is 6.5 nm, which is in good agreement with the expectation that only a monolayer of LH2 was bound to the active ester surface.

**Nanoscale Patterning of LH2 Arrays Using Scanning Near-Field Photolithography.** Conventionally, diffractive pro-

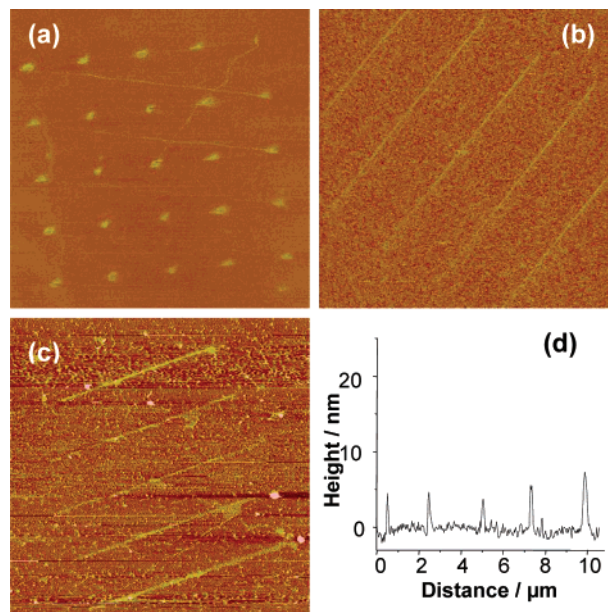


**Figure 4.** AFM images of nanoscale patterns fabricated by SNP: (a)  $12\ \mu\text{m} \times 12\ \mu\text{m}$  FFM image of an array of  $C_{10}COOH$  dots in a  $C_2F_5CF_3$  monolayer ( $z$ -range 0–500 mV); (b)  $15\ \mu\text{m} \times 15\ \mu\text{m}$  FFM image of  $C_{10}COOH$  lines in a  $C_2F_5CF_3$  monolayer ( $z$ -range 0–500 mV); (c)  $15\ \mu\text{m} \times 15\ \mu\text{m}$  tapping mode image of LH2 immobilized onto  $C_{10}COOH$  lines ( $z$ -range 0–40 nm); (d) averaged cross-section across the nanolines in (c) with a mean fwhm of 98 nm.

cesses are thought to limit the resolution of an optical process to approximately half the wavelength of the radiation employed.<sup>40</sup> Recently, however, we have demonstrated that using a scanning near-field optical microscope (SNOM) coupled to a UV laser, an approach termed scanning near-field photolithography (SNP), it is possible to fabricate structures significantly smaller than the conventional diffraction limit.<sup>14–16,18</sup> In SNP, a SAM is exposed to the evanescent electric field associated with a nanometric aperture at the end of an optical fiber probe which is traced across the sample surface using a SNOM. Interaction between the sample and this evanescent field leads to photochemical modification of the adsorbates, yielding sulfonate products that may be displaced by a second thiol to yield chemical patterns that may be as small as 9 nm.<sup>18</sup>

In the present work, monolayers of  $C_2F_5CF_3$  were exposed to UV light from a near-field probe and immersed in a solution of  $C_{10}COOH$ . The samples were then imaged by FFM. Figure 4a and b shows two different types of structure formed this way — an array of dots and a series of parallel lines. Dots were fabricated by exposing the sample to a stationary SNOM probe for 4 s. Lines were fabricated by exposing the sample to a probe that was traveling at a speed of  $0.1\ \mu\text{m}\ \text{s}^{-1}$ . As in the case of the micron-scale structures, the regions in which the fluorinated thiol has been oxidized and replaced by the polar adsorbate exhibit bright contrast because of the larger coefficient of friction associated with the carboxylic acid group. Very narrow diagonal lines may be observed connecting the last point in each row (the one at the left-hand end) with the first point in the row below (the one at the right-hand end) and also joining the initial probe position at the commencement of the lithographic process (the center) with the first feature written (at the upper right-

(36) Carpick, R. W.; Salmeron, M. *Chem. Rev.* **1997**, *97*, 1163.

(37) Frisbie, C. D.; Rozsnyai, L. F.; Noy, A.; Wrighton, M. S.; Lieber, C. M. *Science* **1995**, *265*, 2071.

(38) Kim, H. I.; Koini, T.; Lee, T. R.; Perry, S. S. *Langmuir* **1997**, *13*, 7192.

(39) McDermott, M. T.; Green, J.-B. D.; Porter, M. D. *Langmuir* **1997**, *13*, 2504.

(40) Novotny, L.; Hecht, B. *Principles of Nano-Optics*; Cambridge University Press: Cambridge, UK, 2006; p 95.

hand corner). These were formed because the light source was not blanked during the rapid motions of the probe between locations at which features were to be fabricated (the probe moves ca. 10 times faster than during fabrication of lines as in Figure 4c). Such features indicate that the use of a high scan speed improves the resolution, but the resulting structures are very narrow, and for the present purposes longer exposures were required to ensure ready imaging of the resulting protein patterns.

Carboxylic acid groups introduced to the surface by SNP were converted to active ester functionalities using the same method employed to create the micron-scale pattern in Figure 3b. Following immersion in a solution of monodisperse LH2 complexes solubilized in detergent micelles and then rinsing and drying, the sample was imaged by AFM, in tapping mode, and the image is shown in Figure 4c. The lines are clearly defined, and there is little evidence of nonspecific adsorption of LH2 complexes. To confirm this, a line section analysis was conducted. Figure 4d shows a mean line section across a portion of the image in Figure 4c. Each of the five lines was analyzed at six locations, and the overall mean height was found to be  $6.2 \pm 1.8$  nm, consistent with the formation of a linear monomolecular layer of LH2. The mean full width at half-maximum height (fwhm) was 98 nm. These data indicate that photopatterning by SNP is a very effective means of controlling the adhesiveness of monolayers toward LH2 on length scales approaching molecular dimensions.

**Fluorescence Imaging of LH2 Bound to a Photopatterned Self-Assembled Monolayer.** The principal biological function of LH2 is to form large two-dimensional arrays which collect light and transfer the energy to reaction center-LH1 complexes, where it is converted into a charge separation. It is thus important to establish whether the molecule retains its characteristic optical properties, which are derived from bound bacteriochlorophyll and carotenoid molecules, following immobilization to the patterned surface. Accordingly, the fluorescence emission properties of micron-scale patterns of LH2 were measured using a confocal fluorescence microscope<sup>34</sup> equipped with an avalanche photodiode (APD) and a CCD camera with a monochromator wavelength selector. The sample was illuminated with monochromatic laser light at 800 nm because this coincides with one of the two major absorbance bands of LH2. Light energy is transferred from the B800 to the B850 molecules within the LH2 complex, from which the energy is eventually lost as fluorescence; measurements of fluorescence emission from B850 pigments therefore provide an excellent indication of the retention of the optical activity, and thus structural integrity, of LH2.

Figure 5a shows the fluorescence image recorded using a single photon counting APD, which records light at all wavelengths. Clearly, the immobilized LH2 complexes retain their fluorescent properties, but in order to verify an emission maximum in the near infrared, the CCD camera was used to acquire emission spectra (Figures 5b and 6). The emission spectrum recorded by the CCD of the LH2 complex in solution is shown in Figure 6, spectrum (a), as a reference. The fluorescence emission maximum seen in Figure 6 at  $\sim 820$  nm and present in both areas of the SAM arises from residual broad band emission of the laser diode that passes through the filter and is strongly reflected from the sample surface. A comparison

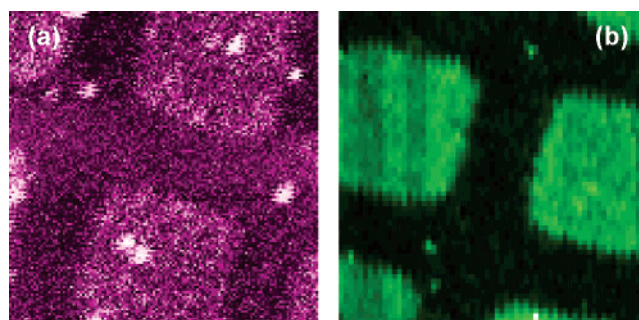


**Figure 5.** False color fluorescence images of LH2 immobilized onto a  $C_2F_5CF_3/C_{10}COOH$  pattern: (a) captured with a single photon counting APD and (b) captured by a prism-based spectrograph. Image sizes: (a)  $23.3 \times 23.3 \mu m$ ,  $128 \times 128$  pixels at 1 ms/pixel; (b)  $23.3 \times 23.3 \mu m$ ,  $64 \times 64$  pixels at 200 ms/pixel. Power at back aperture objective:  $4 \mu W$ .

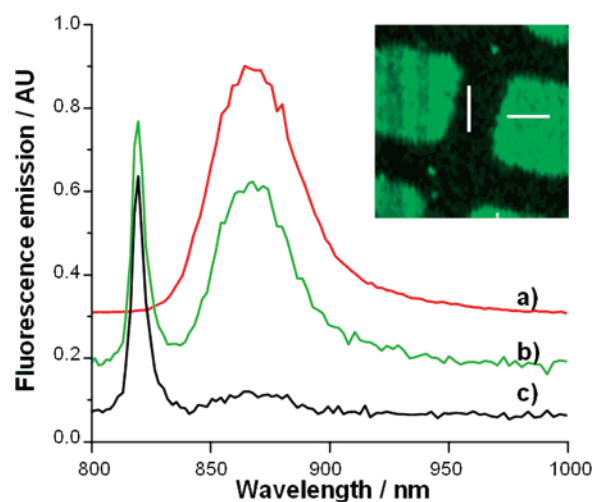


**Figure 6.** (a) Fluorescence emission spectrum of purified LH2 complexes in solution (20 mM Tris, 0.1% LDAO, pH 8.0) recorded at room temperature using the CCD camera. (b) Fluorescence emission spectrum of purified LH2 complexes immobilized onto the NHS ester activated regions of a  $C_2F_5CF_3/C_{10}COOH$  pattern on gold. The spectrum was collected from the region marked by a horizontal line in the inset micrograph. (c) Fluorescence spectrum acquired from the  $C_2F_5CF_3$  surface (vertical line in micrograph). Each spectrum is an average of 25 pixels along each line in the inset. The spectra have been offset for clarity.

of the fluorescence in the protein-resistant ( $C_2F_5CF_3$ ) and -activated (NHS) regions of the SAM is shown in Figure 6. In each case, the emission spectrum is an average of 25 pixels along the horizontal white line (NHS region) and the vertical line ( $C_2F_5CF_3$  region); see inset. There is an almost 10-fold increase in fluorescence at  $\sim 870$  nm seen in the NHS regions compared to the  $C_2F_5CF_3$  regions, which indicates that the binding of purified LH2 complexes in specific spatial arrangements has been achieved. The image created from this spectral information (Figure 5b) exhibits excellent contrast between the activated (square) and protein-resistant areas of the sample. The fluorescence images (Figures 5a,b and 6 inset) in conjunction with the spectroscopic data (Figure 6, spectrum (b)) show that the LH2 complex remains functional after covalent attachment to the SAM. The AFM height images presented in Figures 3 and 4 provide further support for the conclusion that the LH2 complex, which is  $\sim 7$  nm in height,<sup>24,25</sup> has been deposited in a specific and controlled manner to form a layer one molecule thick.

This demonstration that a membrane protein complex, in this case the light-harvesting LH2 complex, can be patterned onto

a SAM while retaining its functional properties, opens up the possibility of using both native and mutated LH complexes, coupled to these and other types of surface, in order to create arrays which exhibit controlled, directional energy migration.

### Conclusions

LH2 adsorbs onto carboxylic acid terminated self-assembled monolayers, probably through an electrostatic interactions with the cytoplasmic face of the complex. However, monolayers terminating in oligo(ethylene glycol), methyl, hydroxyl, and perfluorinated groups resist LH2 adsorption. Photopatterning of monolayers of perfluorinated thiols and introduction of carboxylic acid terminated adsorbates provide a convenient means of controlling LH2 adsorption on length scales from tens of microns (using a mask-based process) to less than 100 nm (using scanning near-field photolithography). Fluorescence spectroscopy measurements on LH2 covalently coupled to

carboxylic acid groups patterned in this fashion exhibited strong emission from B850 pigments, with spectra of immobilized proteins being qualitatively identical to those of solution-phase complexes, providing clear evidence for the retention of the optical activity, and thus structural integrity, of LH2. Methodologies based upon near-field photolithography offer great promise for the fabrication of functional, nanostructured assemblies of membrane proteins.

**Acknowledgment.** G.J.L. and S.J. thank the EPSRC and the RSC Analytical Chemistry Trust Fund for their support. N.P.R. thanks the EPSRC for a Life Sciences Doctoral Training Centre Studentship. M.E.-M. and C.O. appreciate support from the nanotechnology network in The Netherlands (NANONED), project number 7124. J.T., J.D.O., and C.N.H. gratefully acknowledge the BBSRC for support.

JA073658M